

# **PIVO: Probabilistic Inverse Velocity Obstacle for Navigation under Uncertainty**

by

Sri sai poonagam Naga Jyotish, Yash Goel, Sai Bhargav Kumar A V S, Madhava Krishna

Report No: IIIT/TR/2019/-1



Centre for Robotics  
International Institute of Information Technology  
Hyderabad - 500 032, INDIA  
October 2019

# PIVO: Probabilistic Inverse Velocity Obstacle for Navigation under Uncertainty

P. S. Naga Jyotish\*, Yash Goel\*, A. V. S. Sai Bhargav Kumar and K. Madhava Krishna

**Abstract**—In this paper, we present an algorithmic framework which computes the collision-free velocities for the robot in a human shared dynamic and uncertain environment. We extend the concept of Inverse Velocity Obstacle (IVO) to a probabilistic variant to handle the state estimation and motion uncertainties that arise due to the other participants of the environment. These uncertainties are modeled as non-parametric probability distributions. In our PIVO: Probabilistic Inverse Velocity Obstacle, we propose the collision-free navigation as an optimization problem by reformulating the velocity conditions of IVO as chance constraints that takes the uncertainty into account. The space of collision-free velocities that result from the presented optimization scheme are associated to a confidence measure as a specified probability. We demonstrate the efficacy of our PIVO through numerical simulations and demonstrating its ability to generate safe trajectories under highly uncertain environments.

## I. INTRODUCTION

Safety is paramount as robots navigate amongst humans and a cornerstone in ensuring safety lies in efficacious modeling of uncertainty. Often uncertainty estimates can be overly conservative resulting in large deviations in the executed trajectory [1], [2]. The keynote lies in formulations of uncertainty that ensure parsimonious trajectories without compromising safety.

In [3] we had come up with an alternate formulation of the popular velocity obstacle [4] that bypassed the need for estimating the robot's state and velocity, yet execute effective collision avoidance maneuvers from successive observations of moving agents. This alternative formulation was coined as the Inverse Velocity Obstacle (IVO). In this paper we extend this to a probabilistic setting and showcase the benefits of the Probabilistic version of the Inverse Velocity Obstacle (PIVO) vis a vis the Probabilistic version of the velocity obstacle (PVO).

### A. Contribution and Main Results

More specifically the paper contributes in the following ways:

- 1) It shows that the IVO is amenable to a probabilistic setting as we cast it into a chance constrained formulation that solves for control actions accounting for and respecting chance constraints. Chance constraints are probabilistic constraints of the form  $\Pr(f(\cdot) >$

\*Both authors contributed equally to this research

P. S. Naga Jyotish, Yash Goel, A. V. S. Sai Bhargav Kumar and K. Madhava Krishna are with Robotics Research Center at International Institute of Information Technology, Hyderabad, India. srisai.poonganam@research.iiit.ac.in, ygoel@me.iitr.ac.in, vseetharam.a@research.iiit.ac.in, mkrishna@iiit.ac.in

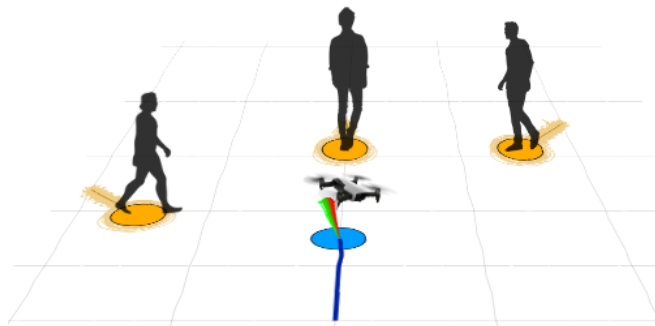


Fig. 1: An illustration of the proposed navigation framework with a robot in human shared environment

- 0)  $> \eta$  which are typically intractable. However they were shown effective in collision avoidance settings by solving for surrogate constraints that are tractable and provide closed form solutions [5], [6], [7].
- 2) Further we show how bypassing the need to estimate the drones ego state results in significant decrease in trajectory lengths without compromising on the safety.
- 3) We show ablation studies that portray the above advantages vis a vis chance constrained formulations that take into account state and velocity noise of the drone/ego-vehicle.
- 4) Further we bypass the need to model uncertainty in a parametric setting even as we model the observation/measurement uncertainties non parametrically and show the efficacy of our formulation in non parametric setting.

It is to be noted that while PIVO characterizes only measurement/observation and control uncertainties, PVO characterizes state, measurement and control uncertainties.

### B. Layout of the paper

The rest of the paper is organized as follows, Section II presents a brief overview of the previous works. Section III introduces to the concept of IVO. In Section IV we present our approach, Probabilistic Inverse Velocity Obstacles and derive its formulation. Section V presents the Path Optimization scheme and the Navigation framework of the proposed work. In Section VI we evaluate our method in different scenarios and present the results compared with the baseline IVO method. We conclude our work in Section 7.

## II. RELATED WORK

In this section, we present a brief overview of the previous works on the robot navigation in human shared environments. Works like Velocity Obstacle [4] are quite popular in the

literature of collision avoidance. Quite a few works like [8], [9], [10] have branched out from the concept of velocity obstacle as an elegant extension in different applications. Our previous work Inverse Velocity Obstacle [3] is one such extension which removes the dependency on self state inferring technique of the autonomous system there by improving the computational complexity significantly. In works like [11][12], extensions to Velocity Obstacles to incorporate car like obstacles were introduced. All the above methods fail to generate collision-free velocities in an uncertain environment.

In [13] the uncertainty associated with the obstacle is handled by modelling it as a Gaussian Process. [14], [1], [2] model the uncertainty as Gaussian random variables parameterized by their mean and co-variance. But these works only consider the uncertainty that arises in the state estimation of other participants and assume a deterministic model for the robot. Being an ego-centric framework our approach eliminates the concept of self-state estimation, which is the drawback in the above presented methods. In [15] the presented algorithm considers both the perception and motion uncertainty but is computationally heavy for calculating tight probability bound at each step.

We also cite the works like [16] that defines the human interaction social norms to develop models. In some approaches [17] they assume the humans as static obstacles or to cooperate with the robots that they share the environment with. The motion planner proposed in [18] generates the trajectory by considering the scenario where all the humans perform their worst possible motion. Learning techniques like [19], [20] with filter tracking and motion models integrated have been implemented that take into account the past error while making the future predictions.

Most of the above methods do not handle uncertainty and even if they do they resort to parametric (Gaussian) models of state, observation and control noise. Instead the proposed formulation contrasts itself by handling non parametric noise models as well as bypassing completely the need to handle state uncertainty. As a consequence of this it shows less conservative trajectories without compromising safety of the interacting agents.

### III. PRELIMINARIES

Throughout this paper, vectors are denoted in bold letters,  $\mathbf{v}$ , matrices in capital,  $M$ .  $\|x\|$  denotes the Euclidean norm of  $\mathbf{x}$ .  $\mu_x$  denotes the mean of a random variable  $x$  and  $\sigma_x$  denotes its standard deviation.  $x_o$  and  $\dot{x}_o$  denote the position and velocity of the obstacle in global frame while  $x_o^r$  and  $\dot{x}_o^r$  denote the position and velocity of the obstacle in the robot's frame.  $x_r$  and  $\dot{x}_r$  denote the position and velocity of the robot in global frame.  $\cdot(t)$  denotes the  $\cdot$  at time  $t$ . The terms  $t + \delta t$  and  $t - \delta t$  refer to the next and previous consecutive time steps of  $t$ .  $\Pr[\cdot]$  denotes the probability of an event and  $p[\cdot]$  denotes a probability density function.

#### A. Inverse Velocity Obstacle

In this section, we briefly review the concept of Inverse Velocity Obstacle (IVO) [3] and how it differs from tradi-

tional Velocity Obstacle. Consider a mobile robot, denoted by  $A$ , and an obstacle, denoted by  $B$ , both taking the shape of a disc of radius  $R_A$  and  $R_B$  respectively. The traditional velocity obstacle for robot  $A$  induced by obstacle  $B$  is the range of velocities of  $A$  that can result in a collision with  $B$  at some point in the future. Here, the robot is reduced to a point while the radius of the obstacle is increased to  $R_A + R_B$ . The collision cone is formed with point robot at its vertex. The inverse velocity obstacle reduces the obstacle to a point object and grows the radius of the robot to  $R_A + R_B$ . The collision cone is formed with the point obstacle at its vertex. It is straight forward from this that the inverse velocity obstacle is the range of velocities of  $B$  that can result in a collision with  $A$  at some point in the future. A graphical representation of collision cones formed with velocity obstacle and inverse velocity obstacle can be found in figure (2). We try to find a new relative velocity of the obstacle which would take the obstacle on a collision free maneuver. We assume that the velocity of obstacle and the robot are instantaneously constant during the time interval  $\delta t$ . This essentially means that the change relative velocity of the obstacle comes from the change in the velocity of the robot. The inverse velocity obstacle is given by

$$f = \|\mathbf{r}\|^2 - (R_A + R_B)^2 - \frac{(\mathbf{r}^T \mathbf{v})^2}{\|\mathbf{v}\|^2} \quad (1)$$

$$\mathbf{r} = \begin{bmatrix} x_o^r(t) \\ y_o^r(t) \end{bmatrix}, \mathbf{v} = \begin{bmatrix} \dot{x}_o^r(t) - u_x \\ \dot{y}_o^r(t) - u_y \end{bmatrix}$$

$[x_o^r(t), y_o^r(t)]^T$  describe the relative position of the obstacle at time  $t$  in the robot's frame of reference.  $[u_x, u_y]^T$  denotes the change in velocity of the robot (or change in relative velocity of the obstacle). The collision avoidance is achieved if the relative velocity vector is outside the collision cone which is given by  $f \geq 0$ . The relative velocity vector can be rewritten in terms of robot's observations as shown in the equation (2).

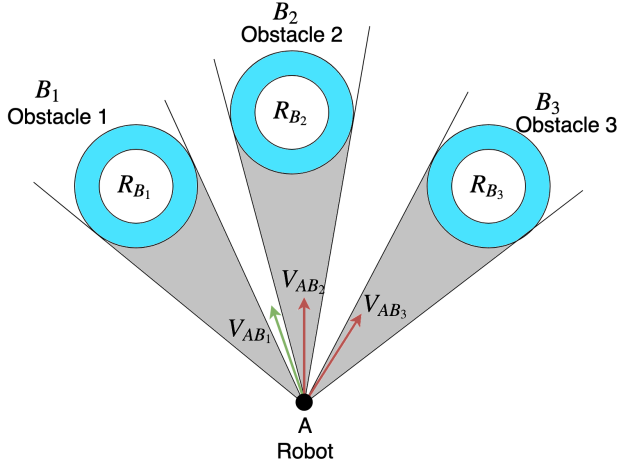
$$\mathbf{v}(t) = \begin{bmatrix} \dot{x}_o^r(t) - u_x \\ \dot{y}_o^r(t) - u_y \end{bmatrix} = \begin{bmatrix} \frac{x_o^r(t) - x_o^r(t - \delta t)}{\delta t} - u_x \\ \frac{y_o^r(t) - y_o^r(t - \delta t)}{\delta t} - u_y \end{bmatrix} \quad (2)$$

The relative position of the obstacles can be directly retrieved from sensor data. Since the collision cone is free from robot's position and velocity estimates, which are usually prone to high magnitudes of noise, one can completely bypass the robot's state estimations for collision detection and avoidance.

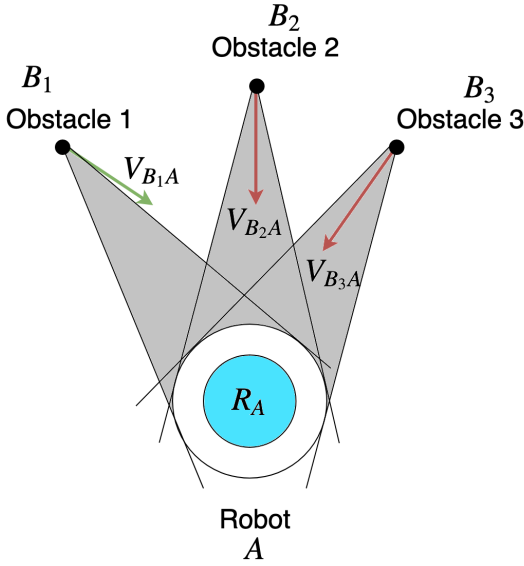
#### B. Chance constraints

Consider a random variable  $x$  that follows an arbitrary distribution and a function  $f(x, \cdot)$ . Assume that  $f(x, \cdot)$  is the function of interest and we want at least  $\eta$  portion of the outcomes of  $f(x, \cdot)$  to be less than  $\lambda$ . This can be expressed in the form of chance constraint as

$$\Pr(f(x, \cdot) < \lambda) \geq \eta$$



(a) Velocity obstacles for three obstacles.



(b) Inverse Velocity obstacles for three obstacles.

Fig. 2: Collision cones formed with VO and IVO. In IVO, the robot is assumed to be at rest while the obstacles move towards it with their respective relative velocities. The green relative velocity lie outside the collision cone and hence not in collision whereas the red ones are in collision.

### C. Uncertainty assumptions

We try to take all uncertainties possible in the formulation. Specifically in the case of IVO, the collision detection and avoidance is invariant to the uncertainty in robot's position and velocity. So, we do not consider the uncertainty in state estimates in our formulation. From equations (1) and (2), it is evident that the collision detection relies on obstacles' position which is prone to sensor noise and the new relative velocity of the obstacle which is effected by the control noise. We assume that the aforementioned uncertainties come from noise models following a non-parametric probability distribution. For the sake of simplicity, we assume that the noise models are independent and their means are zero

centered.

## IV. PROBABILISTIC IVO

### A. Collision avoidance chance constraints

The collision avoidance condition for an obstacle  $i$  of radius  $R_A$  and a robot of radius  $R_B$  in a deterministic case using IVO can be defined as

$$C_i \leq 0 : \frac{(\mathbf{r}^T \mathbf{v})^2}{\|\mathbf{v}\|^2} - \|\mathbf{r}\|^2 + (R_A + R_B)^2 \leq 0$$

$$C_i \leq 0 : \frac{\left( x_o^r(t) \cdot \frac{(x_o^r(t) - x_o^r(t - \delta t))}{\delta t} + y_o^r(t) \cdot \frac{(y_o^r(t) - y_o^r(t - \delta t))}{\delta t} \right)^2}{\left( \frac{(x_o^r(t) - x_o^r(t - \delta t))}{\delta t} \right)^2 + \left( \frac{(y_o^r(t) - y_o^r(t - \delta t))}{\delta t} \right)^2} - (x_o(t)^2 + y_o(t)^2) + (R_A + R_B)^2 \leq 0$$

The terms  $\mathbf{r}$  and  $\mathbf{v}$  are the same as mentioned in equation (1). The collision avoidance chance constraint for the above case is given by

$$\Pr(C_i \leq 0) \geq \eta \quad (3)$$

Here,  $\eta$  the minimum confidence with which we want to avoid the collision. If we were to consider noise, the random variables in this case are  $x_o^r$ ,  $y_o^r$ .

### B. Solving the collision chance constraint

Cantelli's inequality states

$$\Pr(x - \mu_x \geq \beta) \begin{cases} \leq \frac{\sigma^2}{\sigma^2 + \beta^2} & \text{if } \beta > 0 \\ \geq 1 - \frac{\sigma^2}{\sigma^2 + \beta^2} & \text{if } \beta < 0 \end{cases}$$

In our case, we can re-write the inequality as

$$\Pr(C_i - \mu_{C_i} \geq \lambda \sigma_{C_i}) \begin{cases} \leq \frac{1}{1 + \lambda^2} & \text{if } \lambda > 0 \\ \geq 1 - \frac{1}{1 + \lambda^2} & \text{if } \lambda < 0 \end{cases} \quad (4)$$

Using equation (4), the chance constraint in equation (3) can be written as,

$$\Pr(C_i \leq 0 \mid \mu_{C_i} + \lambda \sigma_{C_i} \leq 0) \geq \frac{\lambda^2}{1 + \lambda^2} \quad (5)$$

## V. NAVIGATION UNDER UNCERTAINTY

### A. Path Optimization

Consider a robot at  $\mathbf{x}_r(t)$  moving with a velocity  $\mathbf{v}_r(t)$  towards a goal,  $\mathbf{g}$ . Since the setting of IVO happens to be in a ego-centric frame, let us define a relative goal  $\mathbf{g}^r$  given by

$$\mathbf{g}^r(t) = \mathbf{g} - \mathbf{x}_r(t)$$

In a deterministic case, the new velocity that needs to be taken to reach the goal is given by

$$\mathbf{u}_{opt} = \arg \min_u (\mathbf{v}_d(t - \delta t) + \mathbf{v}_g^r(t - \delta t) - \mathbf{u}(t))^2 \quad (6)$$

$$\mathbf{v}_d(t) = \frac{\mathbf{g}^r(t)}{\|\mathbf{g}^r(t)\|} \cdot v_{max} \quad (7)$$

$$\mathbf{v}_g^r(t) = \frac{\mathbf{g}^r(t) - \mathbf{g}^r(t - \delta t)}{\delta t} \quad (8)$$

Where,  $\mathbf{v}_d$  is the desired velocity which takes the robot towards the goal,  $\mathbf{u}$  is the change in velocity control given to the robot and  $\mathbf{v}_g^r$  is the velocity estimate of the goal with respect to the robot. Let us take a case where the goal is stationary in the global frame. Then the velocity of the robot in the global frame is given by  $\mathbf{v}(t) = -\mathbf{v}_g^r(t)$ . So, for this case, the equation (6) boils down to

$$\mathbf{u}_{opt} = \arg \min_u (\mathbf{v}_d(t - \delta t) - \mathbf{v}(t - \delta t) - \mathbf{u}(t))^2$$

Where  $\mathbf{v}(t)$  is the velocity of the robot in the global frame. The relative positions of the goal in robot's frame can be obtained from a sensor. Since the sensor data can be prone to noise, we alter the cost in equation (6) a little bit to make it robust even in the presence of noise. We perform Monte-Carlo sampling on the modelled parent distribution of sensor noise and define a new cost function based on the sum of squared error between the relative velocity of the goal as seen from the robot,  $\mathbf{v}_{g_i}^r$  (for  $i^{th}$  sample), and  $\mathbf{v}_d$ . The path optimization cost for probabilistic case is given by

$$\mathbf{u}_{opt} = \arg \min_u \sum_{j=1}^M \sum_{i=1}^N (\mathbf{v}_d(t - \delta t) + \mathbf{v}_{g_i}^r(t - \delta t) - \mathbf{u}_j(t))^2 \quad (9)$$

Where,  $\mathbf{v}_{g_i}^r(t)$  and  $\mathbf{u}_j(t)$  are the  $i^{th}$  sample of relative velocity of the goal and  $j^{th}$  sample of control obtained through Monte-Carlo sampling from their respective noise models.

An alternate approach is to obtain an approximate value of  $\mathbf{v}_g^r$  and  $\mathbf{u}$  by taking their respective sample means. In this case, the goal reaching cost is defined using the equation (6).

### B. Navigation framework

The navigation of the robot can be now posed as an optimization problem. Consider the following optimization problem with variables as  $\mathbf{u} = [u_x \ u_y]^T$  which denote the controls given to the robot at time step  $t$ . The goal in robot's frame is given by  $\mathbf{g}^r$  and the maximum attainable velocity of the robot is given by  $v_{max}$ .

$$\min_u \quad J = (\mathbf{v}_d(t - \delta t) + \mu_{v_g^r}(t - \delta t) - \mu_u(t))^2 \quad (10a)$$

$$\text{subject to} \quad \mu_{C_i} + \lambda \sigma_{C_i} \leq 0, \quad \forall i = 1, \dots, N \quad (10b)$$

The terms  $\mu_v$  and  $\mu_u$  in (10a) are the sample means of velocity of the robot and controls given to the robot respectively.  $v_d$  is obtained using equation (7).  $N$  is the number of samples obtained using Monte-Carlo method. We obtain better sample complexity as the value of  $N$  increases. The constraints given by equation (10b) make sure that

$\Pr(C_i) \geq \frac{\lambda^2}{1+\lambda^2} \forall i = 1, \dots, N$  are satisfied. The larger the value of  $\lambda$  is, the higher is the lower bound on confidence of collision avoidance.

## VI. RESULTS

### A. Navigation Under Uncertainty

We show qualitative results of the proposed method in figure (3) where the robot avoids two moving obstacles under observation and control uncertainty. The moving obstacles are shown in a shade of orange with their uncertainty samples giving a noisy visualization. The robot is shown in blue. We show colliding velocity samples of the robot in various shades of red and green. More red implies a large number of velocity samples colliding with a large number of obstacle samples. More green represents a very small fraction, possibly even zero, samples of velocities colliding with very small numbers of obstacle samples. It is to be noted we only compute the change in velocity as the control and not the absolute velocity of the robot. It is purely for illustrative purposes we show velocity samples that are in collision. Figure (3a) depicts the situation when the robot has just avoided the obstacle coming from right and only 34.3% of velocity samples are in collision at that moment, all of which eventually come out as the robot keep moving towards the left.

This soon turns to deep red in figure (3b) wherein all velocity samples collide with most obstacle samples. Due to the computed controls this situation progressively improves from (3c-3d) as green shades progressively dominate. In (3e) and (3f), 82.7% and 29.7% of velocities are in collision respectively and eventually no velocity in collision in (3g). The robot then safely navigates through the two obstacles ensuring no collision to finally reach the goal (3h) through our chance constrained formulation for handling uncertainty.

### B. IVO vs VO

In this section we compare the performance of IVO vs VO. We first compare how they both work in presence of robot state noise in a deterministic setting. By deterministic setting we mean that we do not invoke the chance constrained formulation to compute the robot controls but they are computed through the deterministic IVO formulation. In subsection (VI-B.1) we show while robot state noise alone is present (no observation noise) IVO is superior as it does not need any estimates of its state for computing the avoidance maneuver. Then in subsection (VI-B.2) we compare PIVO vs PVO in a probabilistic framework where robot state noise, obstacle perception noise and control noise is taken into account.

1) *In presence of Robot State Noise:* The uncertainty due to robot state noise is characterized through a gaussian distribution with standard deviation of 0.05 metres with mean as zero. This uncertainty propagates to the state of the moving obstacle mediated by the measurement. Eventually this propagates to the velocity of the moving obstacle when computed as differentiation of states in the classical VO formulation. This uncertainty leads to collisions and longer

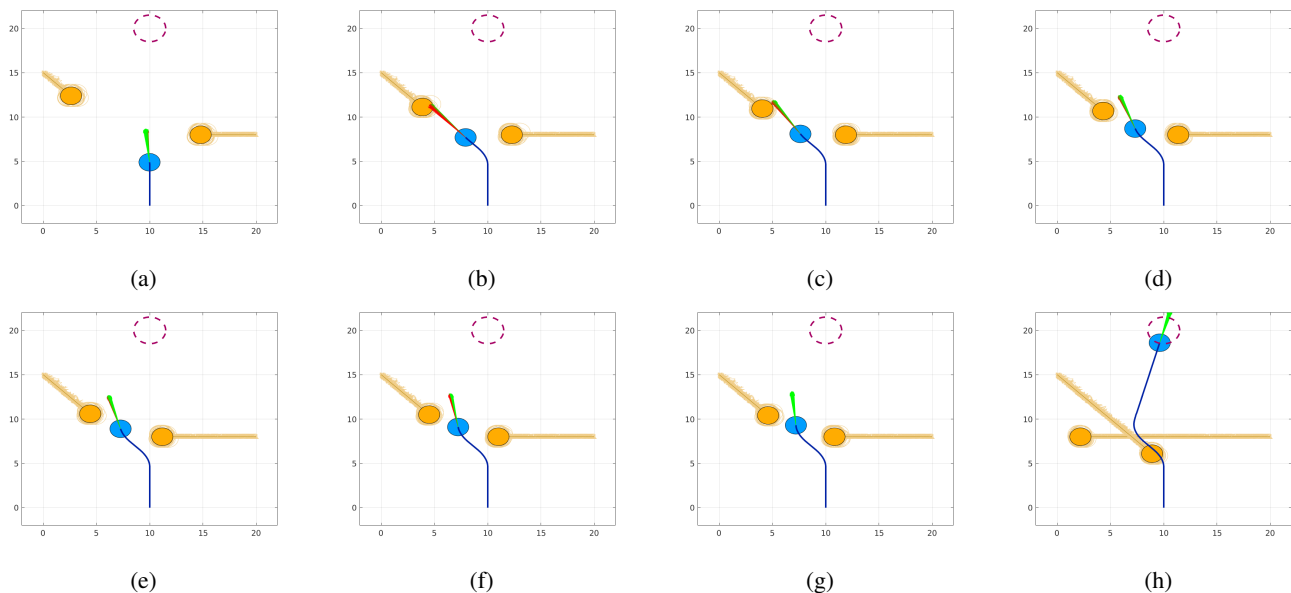


Fig. 3: Collision avoidance sequence considering non-parametric uncertainty. The moving obstacles are shown in a shade of orange with their uncertainty samples while the robot is shown in blue. The velocity samples are shown in shades of green and red depending how many velocity samples are in collision with the obstacle samples.  $x$  and  $y$  axis in the plots denote position ( $m$ ) in  $x$  and  $y$  direction.

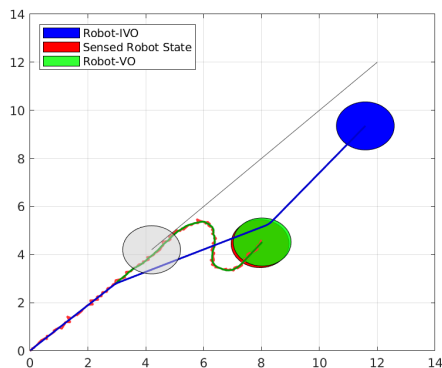


Fig. 4: Deterministic collision avoidance comparison between IVO and VO in presence of robot state noise. The figure demonstrates how IVO is invariant to the noise and manages to avoid collision.  $x$  and  $y$  axis in the plots denote position ( $m$ ) in  $x$  and  $y$  direction.

trajectories of VO agent. Whereas the IVO agent computes the relative velocity of the obstacle with respect to the goal directly from observations bypassing the need to estimate the robot state. This results in collision free trajectories. The VO agent apart from colliding takes a longer path of 25.6859 meters in 29.1 seconds while the IVO agent takes a collision free maneuver towards the goal covering a shorter distance of 22.4833 meters in 23.1 seconds. The figure (4) shows the different trajectories taken in both the cases.

2) *Trajectory Comparison for PIVO vs PVO:* Here we consider a probabilistic framework where uncertainty related to robot state, perception and control is taken. The figure (5)

show the comparison of the trajectories taken by PIVO and PVO for different configurations (5a-5c) whereas the table I quantifies how well the PIVO performs in comparison to PVO for those cases. The PIVO trajectories are shown with orange solid lines while the PVO ones are shown with blue dashed lines. It is to be noted that the PIVO trajectories are less deviant because they are handling lower values of variance in their chance constraints due to their ability to not account for robot state which are noisy to produce collision avoidance manoeuvre. The PIVO trajectories take smaller amount of time to reach the goal while covering a smaller distance as well. For the cases taken here there is an average reduction of 10.73% and 14.06% in the distance travelled and time taken for PIVO in comparison to PVO.

## VII. CONCLUSIONS AND FUTURE WORK

In this work, we presented PIVO an algorithmic framework to handle the uncertain dynamic environment shared by humans using the concept of chance constraints. The presented framework can handle any non-parametric uncertainty and doesn't approximate it to any parametric distribution. Being an ego-centric framework it removes the dependency on the state estimation techniques for inferring the self state there by reducing the computational complexity and aiding for real time implementation. We have evaluated our framework through numerical simulations in different conditions. We show performance gain of PIVO over PVO in terms of trajectory deviation and time while continuing to maintain safety. Our future work include extending the framework for non-holonomic systems.

TABLE I: Trajectory Comparison for  $\lambda = 1.2$ 

Config.	Robot Position Noise ( $m$ ) [ $\sigma_x, \sigma_y$ ]	Robot Velocity Noise ( $ms^{-1}$ ) [ $\sigma_{\dot{x}}, \sigma_{\dot{y}}$ ]	Perception Noise ( $m$ )	Distance Travelled ( $m$ )		Time Taken ( $s$ )	
				IVO	VO	IVO	VO
(a)	[0.6014,0.6939]	[0.2,0.2236]	[0.1902,0.2195]	22.6365	24.8578	13.2	14.6
(b)	[0.6014,0.6939]	[0.2,0.2236]	[0.1902,0.2195]	22.0204	25.1388	11.9	14.1
(c)	[0.6014,0.2195]	[0.4472,0.5477]	[0.1902,0.2195]	15.8772	17.8072	8.3	10.0

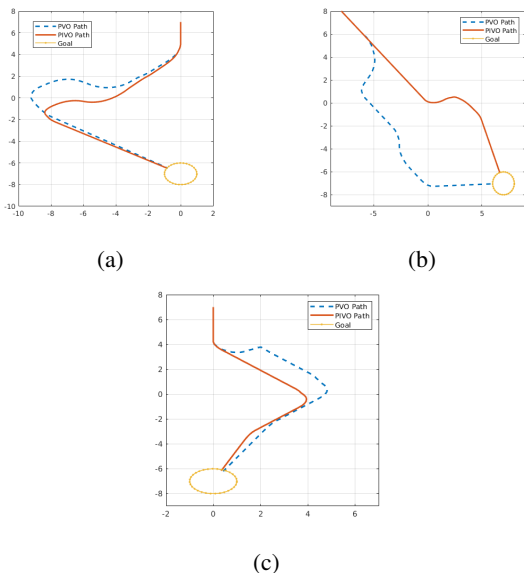


Fig. 5: Trajectory Comparison of VO and IVO. The blue and orange paths are a result of velocity obstacle while the red path is the one taken by the IVO agent. Obstacle trajectories are not shown in these figures for clarity and ease of viewing.  $x$  and  $y$  axis in the plots denote position ( $m$ ) in  $x$  and  $y$  direction.

#### ACKNOWLEDGMENT

This work was supported by Collins Aerospace, IDC.

#### REFERENCES

- [1] J. Snape, J. Van Den Berg, S. J. Guy, and D. Manocha, "The hybrid reciprocal velocity obstacle," *IEEE Transactions on Robotics*, vol. 27, no. 4, pp. 696–706, 2011.
- [2] D. Claes, D. Hennes, K. Tuyls, and W. Meeussen, "Collision avoidance under bounded localization uncertainty," in *2012 IEEE/RSJ International Conference on Intelligent Robots and Systems*. IEEE, 2012, pp. 1192–1198.
- [3] P. S. N. Jyotish, Y. Goel, A. V. S. S. B. Kumar, and K. M. Krishna, "IVO: Inverse Velocity Obstacles for Real Time Navigation," *arXiv e-prints*, p. arXiv:1905.01438, 2019.
- [4] P. Fiorini and Z. Shiller, "Motion planning in dynamic environments using velocity obstacles," *The International Journal of Robotics Research*, vol. 17, no. 7, pp. 760–772, 1998.
- [5] B. Gopalakrishnan, A. K. Singh, and K. M. Krishna, "Closed form characterization of collision free velocities and confidence bounds for non-holonomic robots in uncertain dynamic environments," in *2015 IEEE/RSJ International Conference on Intelligent Robots and Systems (IROS)*, Sep. 2015, pp. 4961–4968.
- [6] B. Gopalakrishnan, A. K. Singh, M. Kaushik, K. M. Krishna, and D. Manocha, "Chance constraint based multi agent navigation under uncertainty," in *Proceedings of the Advances in Robotics*. ACM, 2017, p. 53.
- [7] H. Zhu and J. Alonso-Mora, "Chance-constrained collision avoidance for mavs in dynamic environments," *IEEE Robotics and Automation Letters*, vol. 4, no. 2, pp. 776–783, 2019.
- [8] A. K. Singh and K. M. Krishna, "Reactive collision avoidance for multiple robots by non linear time scaling," in *52nd IEEE Conference on Decision and Control*. IEEE, 2013, pp. 952–958.
- [9] B. Gopalakrishnan, A. K. Singh, and K. M. Krishna, "Time scaled collision cone based trajectory optimization approach for reactive planning in dynamic environments," in *2014 IEEE/RSJ International Conference on Intelligent Robots and Systems*. IEEE, 2014, pp. 4169–4176.
- [10] A. S. B. Kumar, A. Modh, M. Babu, B. Gopalakrishnan, and K. M. Krishna, "A novel lane merging framework with probabilistic risk based lane selection using time scaled collision cone," in *2018 IEEE Intelligent Vehicles Symposium (IV)*. IEEE, 2018, pp. 1406–1411.
- [11] J. Van Den Berg, J. Snape, S. J. Guy, and D. Manocha, "Reciprocal avoidance with acceleration-velocity obstacles," in *2011 IEEE International Conference on Robotics and Automation*. IEEE, 2011, pp. 3475–3482.
- [12] J. Alonso-Mora, A. Breitenmoser, P. Beardsley, and R. Siegwart, "Reciprocal collision avoidance for multiple car-like robots," in *2012 IEEE International Conference on Robotics and Automation*. IEEE, 2012, pp. 360–366.
- [13] C. Fulgenzi, C. Tay, A. Spalanzani, and C. Laugier, "Probabilistic navigation in dynamic environment using rapidly-exploring random trees and gaussian processes," in *2008 IEEE/RSJ International Conference on Intelligent Robots and Systems*. IEEE, 2008, pp. 1056–1062.
- [14] B. Kluge and E. Prassler, "Recursive probabilistic velocity obstacles for reflective navigation," in *Field and Service Robotics*. Springer, 2003, pp. 71–79.
- [15] B. Luders, M. Kothari, and J. How, "Chance constrained rrt for probabilistic robustness to environmental uncertainty," in *AIAA guidance, navigation, and control conference*, 2010, p. 8160.
- [16] E. T. Hall, "The hidden dimension, doubleday & co," *Garden City: New York*, 1966.
- [17] T. Kruse, A. K. Pandey, R. Alami, and A. Kirsch, "Human-aware robot navigation: A survey," *Robotics and Autonomous Systems*, vol. 61, no. 12, pp. 1726–1743, 2013.
- [18] H. Li, O. A. I. Ramirez, and M. Chetouani, "Potential human reaction aware mobile robot motion planner: Potential cost minimization framework," in *The 23rd IEEE International Symposium on Robot and Human Interactive Communication*. IEEE, 2014, pp. 441–448.
- [19] M. Kuderer, H. Kretschmar, C. Sprunk, and W. Burgard, "Feature-based prediction of trajectories for socially compliant navigation," in *Robotics: science and systems*, 2012.
- [20] P. Trautman, J. Ma, R. M. Murray, and A. Krause, "Robot navigation in dense human crowds: Statistical models and experimental studies of human-robot cooperation," *The International Journal of Robotics Research*, vol. 34, no. 3, pp. 335–356, 2015.